Diffusion modeling of recessional flow on central Amazonian floodplains

Douglas Alsdorf,[1] Thomas Dunne,[2,3] John Melack,[2,3] Laurence Smith,[4] and Laura Hess[3]

Received 17 August 2005; revised 19 September 2005; accepted 4 October 2005; published 5 November 2005.

[1] We present a continuity-based approach for calculating flow delivered to a main channel from an adjacent floodplain and use the values in a linear diffusion model to generalize fluxes across a floodplain. Using interferometric synthetic aperture radar (SAR) measurements of floodplain water level changes and the continuity equation, we demonstrate that flow rates are not the same throughout Amazonian floodplains. Also, rates of floodplain storage change are found to be least in areas of greatest distance from a main channel which suggests a long residence time. Linear diffusion modeling of floodplain drainage represents the composite behavior of flow through channels, swamps and lakes and provides a simple method of defining storage changes. The key parameter necessary for diffusion modeling is floodplain conductivity which can be constrained by a simple description of floodplain topography and measurements of temporal changes in floodplain water levels. **Citation:** Alsdorf, D., T. Dunne, J. Melack, L. Smith, and L. Hess (2005), Diffusion modeling of recessional flow on central Amazonian floodplains, *Geophys. Res. Lett.*, *32*, L21405, doi:10.1029/2005GL024412.

1. Introduction

[2] Floodplain inundation and drainage are important components of the sources and routing of flood waves along lowland river valleys. For example, based on Muskingum modeling, *Richey et al.* [1989] estimated that the Amazon mainstem exchanges about 25% of its average annual flow with the floodplain. It is difficult to measure the elevation of floodwaters over an entire floodplain, and especially to measure changes in water levels that contribute to the flux between a main channel and its floodplain. Thus, to estimate mass balances during the passage of a flood wave, the usual model of floodplain inundation and drainage envisions the water surface as horizontal and equal to the changing level of water in the axial channel [e.g., *Richey et al.*, 1989].

[3] Recent work has shown that the situation is more complex [*Mertes*, 1997] and indicates the value of characterizing the spatial and temporal change of water surface elevations during both the inundation and drainage phases of flood seasons. For example, *Alsdorf et al.* [2000] used interferometric SAR measurements of water level changes across the central Amazon floodplain (i.e., $\partial h/\partial t$ where h is the floodplain water surface elevation and t is time) to show that the field of h values is not horizontal and $\partial h/\partial t$ values are not equivalent to the associated main channel. *Alsdorf* [2003] spatially integrated the $\partial h/\partial t$ values to suggest that floodplain storage change errors of 30% may occur when assuming a horizontal water surface – a large error when considering the vastness of the Amazon floodplain.

[4] In this paper, we use interferometric SAR observations in the context of the continuity equation to construct hydrologic flux balances for select reaches of the Amazon, Purús and Negro floodplains in the central Amazon Basin. Variations amongst the flux balances allow us to describe the recessional flows. The $\partial h/\partial t$ values, combined with the flux balances, are then used in a linear diffusion hydraulic model of floodplain storage.

2. Floodplain Geomorphology and Hydrology

[5] The geomorphology of the Amazon and Purús reaches is distinct from that of the Negro (Figure 1). The Amazon and Purús rivers are surrounded by broad, low relief expanses that are inundated at the peak of the flood wave (~10 m). We consider the floodplains of the Amazon and Purús reaches as those areas that are inundated as indicated in Figure 1 (floodplain area, A_f, Table 1). They are bounded by land which is not flooded, called terra firme. Lakes ranging widely in size and shape abound on the floodplain [*Sippel et al.*, 1992] and channels of various widths, depths, and degrees of boundary definition convey water along convoluted paths. Drainage across this complex landscape can be further impeded by floating grasses, trees and organic debris.

[6] In contrast, the lower Negro River lacks a large floodplain coupled with a single main channel (Figure 1). Flow is directed through a 15 km wide archipelago consisting of 500 m to 2000 m wide channels and islands. Terra firme uplands border the archipelago with elevations exceeding 40 m resulting in comparatively less inundated area per unit channel length than is found in the Amazon or Purús reaches (A_f/L_f Table 1, L_f is reach length,). Most of the inundated area along the Negro consists of *ria* lakes located between a river channel and adjacent terra firme [*Sippel et al.*, 1992] and we refer to this area as the Negro floodplain. These lakes are well defined in the SAR imagery such that flow delivered to the Negro River across

[1]Department of Geological Sciences, Ohio State University, Columbus, Ohio, USA.
[2]Donald Bren School of Environmental Science and Management, University of California, Santa Barbara, California, USA.
[3]Institute for Computational Earth System Science, University of California, Santa Barbara, California, USA.
[4]Department of Geography, University of California, Los Angeles, California, USA.

0094-8276/05/2005GL024412$05.00

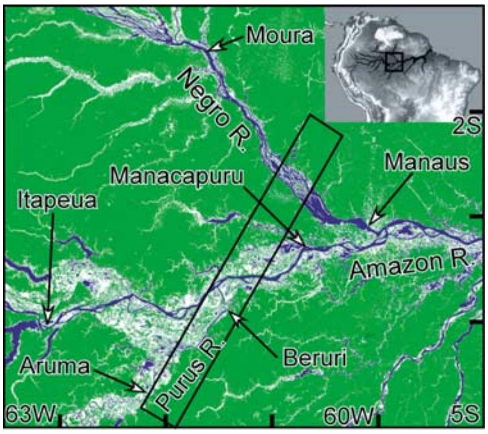

Figure 1. Overlay of two mosaics of JERS-1 L-band SAR images over the central Amazon Basin acquired during the low-water period of late 1995 and during peak stage in 1996 [*Rosenqvist et al.*, 2002]. White marks annually inundated areas; dark blues are always flooded; green is indicative of non-flooded areas [*Hess et al.*, 2003]. Diagonal box locates the interferometric SIR-C swath of *Alsdorf et al.* [2000]. Gauge locations are marked with arrows, study reaches span between gauges (Purus reach extends past Beruri to the mouth).

its floodplain appears in defined paths that are distinct from each other.

3. Recessional Flow Hydrology

[7] The simplified, hydrologic flux balance of the Amazon, Purús, and Negro floodplains is presented in equation (1) and Figure 2:

$$\Delta S_f = Q(0,t) - \mathrm{q} - \mathrm{Q}(\mathrm{x_L},\mathrm{t}) \qquad (1)$$

where rate of change in floodplain storage is ΔS_f, flow delivered to a main channel from the adjacent floodplain is $Q(0,\ t)$, q is the difference between precipitation P and evaporation E, and flow to a floodplain from the adjacent terra firme is $\mathrm{Q(x_L,\ t)}$. All terms have dimensions of length^3/time. Infiltration is neglected in equation (1) whereas upstream floodway inputs and downstream outflows are assumed to balance.

[8] The rate of change in floodplain storage, ΔS_f, is derived from measurements of changes in water levels, $\partial h/\partial t$, following *Alsdorf* [2003]. The NASA Space Shuttle acquired two overlapping swaths of SAR data on October 9 and 10, 1994 (the SIR-C mission), which yielded one-day interferometric measures of $\partial h/\partial t$ distributed across portions of all three study reaches [*Alsdorf et al.*, 2000]. In Figure 3, trends drawn through the $\partial h/\partial t$ values are regarded as functions that describe the water level change throughout a floodplain for the recessional flow. Thus each floodplain reach is treated as having a smoothly changing $\partial h/\partial t$ with distance (local variations are likely more complex). *Alsdorf* [2003] used these trends to estimate ΔS_f of the Amazon floodplain reach as 4600 m^3/s (+400 m^3/s, −900 m^3/s). Here, we use the same method to estimate ΔS_f for the Purús and Negro floodplains (1700 +440, −420 m^3/s and 850 +250, −200 m^3/s, respectively, $\Delta S_f/\mathrm{L_f}$ Table 1). These are the first measurements of Amazon ΔS_f.

Table 1. Floodplain Reach Areas, Lengths, and Water Fluxes[a]

Reach	$\mathrm{A_f}$	$\mathrm{L_f}$	$\mathrm{A_f/L_f}$	$\Delta \mathrm{S_f/L_f}$	$\mathrm{q/L_f}$	$\mathrm{Q(X_L,\ t)/L_f}$	$\mathrm{Q(0,\ t)/L_f}$
Amazon	11800	310	38	15	0.45	2.2	18
Purus	6000	190	32	8.9	0.36	2.2	12
Negro	2000	280	7.1	3.0	0.082	2.2	5.3

[a]Notes: Areas determined from *Hess et al.* [2003] image classifications. Nomenclature follows text: $\mathrm{A_f}$ in km^2; $\mathrm{L_f}$ in km; $\mathrm{A_f/L_f}$ in km^2/km; others in m^3/s/km.

[9] The term q equals P-E integrated over the reach area. At six gauging locations within ∼100 km of the SIR-C swath, the daily average rainfall from July peak stage to October was 4.6 mm/day. Assuming a typical evaporation rate of 3.6 mm/day for the area [e.g., *Costa and Foley*, 1999], we set q at 1.0 mm/day or 140 m^3/s, 69 m^3/s, and 23 m^3/s for the Amazon, Purús, and Negro study reaches, respectively ($\mathrm{q/L_f}$ Table 1).

[10] The inflow from terra firme surrounding a floodplain, $\mathrm{Q(x_L,\ t)}$, is estimated from rainfall-runoff data. For example, flow from the terra firme to the Amazon floodplain in the Itapeua to Manaus reach was estimated by *Richey et al.* [1989] and *Dunne et al.* [1998] to range from 1200 m^3/s in July to 500 m^3/s in October; we use the average of 690 m^3/s for $\mathrm{Q(x_L,\ t)}$ in each study reach ($\mathrm{Q(x_L,\ t)/L_f}$ Table 1). We assume that inflows from terra firme surrounding the Purús and Negro floodplains are similar to these model derived values for the Amazon floodplain.

[11] The flow delivered to a main channel from an adjacent floodplain is calculated from equation (1). During mid-recessional flow in October 1994, we obtained $Q(0,\ t)$ values of 5500 m^3/s, 2200 m^3/s, and 1500 m^3/s for the Amazon, Purús, and Negro study reaches, respectively ($Q(0,\ t)/\mathrm{L_f}$ Table 1). In the previous paragraphs, the time periods used for deriving each equation (1) quantity differ, thus these $Q(0,\ t)$ values are intended as approximations for average recessional flow conditions.

[12] The interferometric observations in Figure 3 are the $\partial h/\partial t$ term in the mass continuity equation [e.g., *Dingman*, 1984],

$$\frac{\mathrm{q}}{\mathrm{W_f}} - \frac{\partial Q}{\partial x} = \mathrm{L_f}\frac{\partial h}{\partial t} \qquad (2)$$

where $\mathrm{L_f}$ is the dimension perpendicular to the direction of floodplain flow (i.e., generally parallel to main channel flow and assumed to be equivalent to the reach length), x is a location anywhere between the floodplain boundaries, and $\mathrm{W_f}$ is the total distance between boundaries (Figure 2).

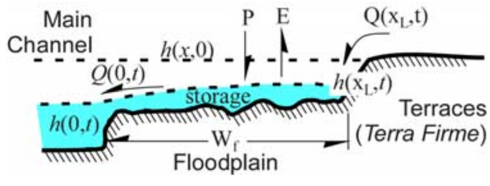

Figure 2. Schematic cross-section of complex, floodplain geomorphology showing components in the water flux-balance along the flow paths noted in Figure 3. Nomenclature follows text.

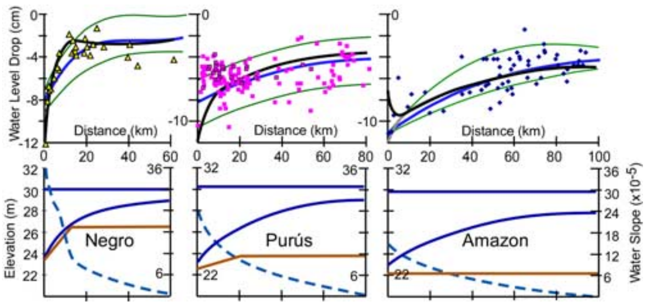

Figure 3. Interferometrically measured water level decreases (dots) from October 9 to 10, 1994 plotted with respect to flow path distance from their major river. See *Alsdorf* [2003] for method of delineating distance. Zero-distance drops are gauge data. Trends drawn through drops are used to estimate floodplain storage changes (blue lines) and errors (green lines). Black lines indicate linear diffusion model fits of predicted $\partial h/\partial t$ from October 9 to 10. Amazon plot includes model changes from October 8 to 9 (grey line). Bottom plots detail simple model floodplain topography (brown line, left ordinate), water surfaces on July 1 (uppermost blue line) and October 10 (lowermost blue line), and gradients of October 10 water surface (dotted blue line, right ordinate).

[13] For the 50 days prior to the SIR-C acquisitions, the main channels of the Amazon, Purús, and Negro rivers were dropping an average of 10.1, 10.2 and 9.2 cm/day (Table 2), respectively, after a total decrease in stage from early July of 6.9, 7.0, and 6.5 m, respectively. If water storage change rates in a floodplain achieved a steady rate of flow resulting in a constant $\partial Q/\partial x$ in equation (2), then this rate should eventually equally affect both proximal and distal portions of a floodplain causing $\sim$9–10 cm/day drops at all distances. However, the interferometric observations in Figure 3 demonstrate that drops greater than 8 cm are typically found within $\sim$30 km of either the Purús or Amazon rivers (and only within the Negro archipelago) whereas beyond $\sim$30 km distance, the drops are almost exclusively less than 8 cm.

[14] In Figure 3, the increasing magnitude of $\partial h/\partial t$ with decreasing distance from a main river channel (x in equation (2)) demonstrates that proximal floodplain storage change rates are greater than distal rates (based on our one-day $\partial h/\partial t$ measurements). Assuming q and L_f in equation (2) are constant across an individual reach, the $\partial h/\partial t$ trends indicate that each study reach contains a drainage imbalance with increasing Q per unit x distance approaching a main channel. The alternative of a sudden increase in main channel drop rates resulting in an increased proximal floodplain $\partial h/\partial t$ is not possible given the gauge values of Table 2. This further implies that water residence times per unit width (unit x) are longer in distal floodplain areas than in river-proximal areas. However, the decreasing trend for the Purús floodplain cannot be as clearly defined as those of the Amazon and Negro reaches. Nevertheless, Purús floodplain $\partial h/\partial t$ values are consistently less than its main channel, indicating that, like the Amazon and Negro, the assumptions of a horizontal h and equivalence of $\partial h/\partial t$ values between channels and floodplains, which are built into one-dimensional flow routing, are in question.

4. A Linear Diffusion Flow Model

[15] We seek a simple model with limited parameterization to describe the broad features of floodplain storage and drainage. The model should be capable of incorporation in continental-scale water cycle models yet capture the basics of complex floodplain flow. The flow paths across the Amazon and Purús floodplains pass a volume of water moving through a myriad of channels and lakes with associated flooded forests and floating plants. We propose to represent the collective behavior of the water in these flow paths with a linear diffusion equation. Although flow across the Negro floodplain involves more discrete, less extensive flow paths, we apply the diffusion model there for comparisons.

[16] Previous uses of diffusion based modeling of floodplain flow have relied on high resolution digital elevation data (1 to 100 m^2 grid cells) and non-linear flow equations [*Makhanov et al.*, 1999; *Lal*, 1998] to predict discharge, water depths and inundation extent. The model results generally matched gauge derived discharge and remote sensing measurements of inundation extent over small floodplains [*Bates and De Roo*, 2000], but only *Makhanov et al.* [1999] attempted to match temporal variations in water heights across a floodplain. We use the following one-dimensional, simple relationship to describe Q:

$$Q(x,t) = -\mathrm{KL_f}h\frac{\partial h}{\partial x} \qquad (3)$$

where K is floodplain conductivity, $L_f h$ is the cross-sectional area perpendicular to the floodplain flux, and $Q(x, t)$ is the flow across a floodplain (i.e., the x direction in Figure 2). Substituting equation (3) into the mass continuity equation (equation (2)) yields the following equation of flow:

$$\frac{\mathrm{q}}{\mathrm{W_f L_f}} + \mathrm{K}h\frac{\partial^2 h}{\partial x^2} = \frac{\partial h}{\partial t} \qquad (4)$$

Equation (1) expresses the relationship between changes in floodplain storage and the boundary flow terms indicated in Figure 2 which are necessary for solving equation (4).

[17] We developed a one-dimensional finite difference model to solve equation (4). The boundary conditions include a main channel with its water height, $h(0, t)$, decreasing with time (i.e., measured from a gauge, Table 2), and an upland margin with a boundary inflow term ($Q(x_L, t)$ in Figure 2 and Table 1). For the initial conditions at peak stage in early July we assume that the water surface across the floodplain, $h(x, 0)$ in Figure 2, is

Table 2. Daily Changes in Main Channel Water Levels, 1994[a]

River	Gauge	Oct 10–9	Oct 9–8	Oct 10–4	Oct 10–Aug 20
Negro	Moura	−6	−9	−11.3	−7.1
Negro	Manaus	−12	−12	−12.0	−9.2
Amazon	Itapeau	−5	−5	−7.0	−10.1
Amazon	Manacapuru	−7	−13	−11.1	−10.1
Purus	Beruri	−12	−14	−10.4	−10.2

[a]Notes: Drops in cm. Oct. 10 minus Oct. 4 changes (one week) and Oct. 10 minus Aug. 20 changes (half of the 101 days since peak stage) are an average of the encompassed one-day decreases.

equivalent to the stage in the main channel. Subtracting the bottom topography from h, yields an average depth of floodplain flow at every x and t node. Therefore, in this application of equation (4), h is a function of x and t, while K, q, and L_f are held constant.

[18] The two unknown parameters in equation (4), K and the general elevation of the floodplain surface, can be found by simultaneously (a) fitting the storage change predicted from equations (4) and (1) to the interferometric value of ΔS_f and (b) fitting the daily differences in water heights derived from equation (4) to the interferometrically observed drops in water level (Figure 3). We used the Manacapurú gauge data for the main-channel boundary condition to model the flow across the Amazon floodplain between Itapeua and Manacapurú. Setting the elevation of the floodplain to a horizontal plane results in a model prediction that matches the interferometric observations and corresponding storage change estimate with a conductivity of 12800 km/day.

[19] To model the Purús floodplain reach between Aruma and the confluence with the Amazon, we used the Beruri gauge data and found that a ramp-and-flat bottom topography was necessary (Figure 3). The use of a horizontal plane in the Purús model resulted in predicted $\partial h/\partial t$ values that either (a) matched the main channel but were more negative than the interferometric observations on the floodplain or (b) matched the floodplain but were less negative than the main channel water level change. The Purús floodplain diffusion model produces an approximate fit to both the drops and storage change with predicted K value of 6500 km/day, but notable differences do occur near the Purús channel. Water surface changes measured near the channel are smaller than predicted probably because the one-dimensional flow model does not include water forced overbank further upstream by backwater effects of the Amazon on the Purús [*Meade et al.*, 1991]. For comparisons with the two larger floodplains, we also applied the diffusion model to the smaller Negro floodplain. Here, a steeper ramp than the Purús was required to fit the observations and a conductivity of 8500 km/day was derived.

[20] In this application of the diffusion equation, floodplain conductivity encompasses the effect on flow from various floodplain characteristics such as inundated area (some fraction of the floodplain may not be inundated), the topography created by various geomorphic features, channels of various sizes that fret the floodplain, and vegetation. Local variations in depths are also incorporated by the tradeoff between K and our use of general floodplain topography, wherein increasing the bottom slope and decreasing K can be used to maintain a constant $Q(0, t)$. Because the three reaches have low topographic relief, we designed their diffusion models to maintain the lowest trans-floodplain gradients possible while still matching the interferometric observations. An indication of the relationship between conductivity and daily main channel height changes can be found by comparing predicted floodplain $\partial h/\partial t$ values for two separate 24 hour periods (Figure 3, Amazon plot). From October 8 to 9 the mainstem stage declined 13 cm whereas from October 9 to 10 it dropped only 7 cm (Table 2). With a conductivity of 12800 km/day, the model predicts that this variation will penetrate about 10 km into the Amazon floodplain in one day. Because multi-temporal interferometric measurements of water level changes are possible using JERS-1 data [*Alsdorf et al.*, 2001], future work will determine if K is constant for a particular floodplain reach or varies with main channel stage.

5. Conclusions

[21] Using just two parameters, conductivity and a basic description of floodplain topography, the 1D, linear-diffusion model is a simple method of characterizing complex floodplain flow. This approach revises the theoretical model employed in continental-scale water cycle models where water level changes in the main channel are instantly propagated laterally across the entire floodplain to one where this elevation change propagates across the floodplain as a 1D diffusion wave. The model captures the fundamental behavior of recessional flow as measured by satellite interferometric SAR.

[22] **Acknowledgments.** Funded by NASA's programs in SENH and THP (DEA), LBA (JMM, TD) and EOS (TD). Manny Gabet helped develop the diffusion model code and Paul Bates provided a key review.

References

Alsdorf, D. E. (2003), Water storage of the central Amazon floodplain measured with GIS and remote sensing imagery, *Ann. Assoc. Am. Geogr.*, *93*, 55–66.

Alsdorf, D. E., J. M. Melack, T. Dunne, L. A. K. Mertes, L. L. Hess, and L. C. Smith (2000), Interferometric radar measurements of water level changes on the Amazon floodplain, *Nature*, *404*, 174–177.

Alsdorf, D., C. Birkett, T. Dunne, J. Melack, and L. Hess (2001), Water level changes in a large Amazon lake measured with spaceborne radar interferometry and altimetry, *Geophys. Res. Lett.*, *28*, 2671–2674.

Bates, P. D., and A. P. J. De Roo (2000), A simple raster-based model for flood inundation simulation, *J. Hydrol.*, *236*, 54–77.

Costa, M. H., and J. A. Foley (1999), Trends in the hydrologic cycle of the Amazon basin, *J. Geophys. Res.*, *104*, 14,189–14,198.

Dingman, S. L. (1984), *Fluvial Hydrology*, W. H. Freeman, New York.

Dunne, T., L. A. K. Mertes, R. H. Meade, J. E. Richey, and B. R. Forsberg (1998), Exchanges of sediment between the flood plain and channel of the Amazon River in Brazil, *Geol. Soc. Am. Bull.*, *110*, 450–467.

Hess, L. L., J. M. Melack, E. M. Novo, C. Barbosa, and M. Gastil (2003), Dual-season mapping of wetland inundation and vegetation for the central Amazon basin, *Remote Sens. Environ.*, *87*, 404–428.

Lal, A. M. W. (1998), Performance comparison of overland flow algorithms, *J. Hydraul. Eng.*, *124*, 342–349.

Makhanov, S. S., S. Vannakrairojn, and E. J. Vanderperre (1999), 2D numerical model of flooding in east Bangkok, *J. Hydraul. Eng.*, *125*, 407–414.

Meade, R. H., J. M. Rayol, S. C. Da Conceicao, and J. R. G. Natividade (1991), Backwater effects in the Amazon River basin of Brazil, *Environ. Geol. Water Sci.*, *18*, 105–114.

Mertes, L. A. K. (1997), Documentation and significance of the perirheic zone on inundated floodplains, *Water Resour. Res.*, *33*, 1749–1762.

Richey, J. E., L. A. K. Mertes, T. Dunne, R. L. Victoria, B. R. Forsberg, A. C. N. S. Tancredi, and E. Oliveira (1989), Sources and routing of the Amazon River flood wave, *Global Biogeochem. Cycles*, *3*, 191–204.

Rosenqvist, A., M. Shimada, B. Chapman, L. Dutra, and S. Saatchi (2002), The Global Rain Forest Mapping project: Introduction from the guest editors, *Int. J. Remote Sens.*, *23*(7), 1215.

Sippel, S. J., S. K. Hamilton, and J. M. Melack (1992), Inundation area and morphometry of lakes on the Amazon River floodplain, Brazil, *Arch. Hydrobiol.*, *123*, 385–400.

D. Alsdorf, Department of Geological Sciences, Ohio State University, 125 South Oval Mall, Columbus, OH 43210, USA. (alsdorf.1@osu.edu)

T. Dunne and J. Melack, Donald Bren School of Environmental Science and Management, 2400 Bren Hall, University of California, Santa Barbara, CA 93106-5131, USA.

L. Hess, Institute for Computational Earth System Science, University of California, Santa Barbara, CA 93106, USA.

L. Smith, Department of Geography, University of California, Los Angeles, CA 90095, USA.